CHARACTERIZATION OF HYDROLYTIC DEGRADATION OF U-F JOINTS THROUGH APPARENT DIFFUSIVITY

Jae Sik Na

Didier Ronze

and

André Zoulalian

LERMAB—Equipe Génie des Procédés
ENSTIB—Université Henri Poincaré, Nancy 1 BP 239
54506 Vandœuvre les Nancy CEDEX, France

(Received January 1996)

ABSTRACT

The hydrolytic aging of an adhesive joint (wood-urea/formaldehyde resin) is characterized by measurements of the apparent diffusivity of two inert gases within the bond. This kind of measurement is of some interest, because it includes both chemical and geometrical changes in joint structure.

Apparent diffusivities are determined in a diffusion cell after various degradation times in a cold water bath. Our results show that diffusivity increases with aging time with an asymptotic trend. Nevertheless, when the joint undergoes cyclic aging (immersion/drying), chemical degradation occurs mainly during the first cycle, while mechanical degradation observed during the drying steps also appears during the following cycles. The values of apparent diffusivity show that the solute transport is a real diffusional transport phenomenon and that resin joints are not porous.

Keywords: Urea-formaldehyde, hydrolysis, aging, diffusivity, chemical degradation, mechanical degradation.

NOTATIONS

C_{A1}	concentration of A in cell 1 (mole·m^{-3})
C_{A2}	concentration of A in cell 2 (mole·m^{-3})
C^0_{A1}	initial concentration of A in cell 1 (mole·m^{-3})
C^0_{A2}	initial concentration of A in cell 2 (mole·m^{-3})
d	pore diameter (m)
D	diffusion coefficient (m^2·s^{-1})
$\mathbb{D}$	apparent diffusivity (m^2·s^{-1})
e	thickness of the sample (m)
k_1	local transfer coefficient in cell 1 (m·s^{-1})
k_2	local transfer coefficient in cell 2 (m·s^{-1})
K	global transfer coefficient (m·s^{-1})
Kn	Knudsen number (−)
m	partition coefficient (−)
M	(kg·mole^{-1})
R	gas constant (J·mole^{-1}·K^{-1})
S	transfer area of the sample (m^2)
T	absolute temperature (K)
V_1	volume of cell 1 (m^3)
V_2	volume of cell 2 (m^3)
ΔP	pressure drop (Pa)
λ	mean free path of the gas molecules (m)
σ	molecular radius (m)
Φ_A	specific flow of solute A (mole·m^{-2}·s^{-1})

INTRODUCTION

The urea-formaldehyde/wood joints commonly used for wood structures may deteriorate under some conditions and lead to the rupture of these works. Thus it seems impor-

Wood and Fiber Science, 28(4), 1996, pp. 411–421

tant to be able to qualify and/or quantify the urea-formaldehyde (UF) resin's durability as an important criterion of the joint quality, but not the only one.

Durability is linked mainly to the hydrolytic cleavage of joints in wood-UF systems (chemical degradation) and to the stresses due to dimensional variations (shrinkage-swelling) of wood when the moisture content varies (mechanical degradation).

Hydrolysis can occur at many sites in the UF resin structure (Myers 1982) and is enhanced in hot acid medium. It can be measured approximately through formaldehyde release (Troughton and Chow 1975; Myers 1990); however, such a release can be strongly decreased because of wood-formaldehyde interactions and diffusion effects. Furthermore, interfacial bonds (hemiformal, formal, N-methylol, . . .) are very sensitive to hydrolysis and thus also take part in formaldehyde release.

The steep moisture gradients encountered during some uses of UF joints lead to shrinkage-swelling phenomena, which induce deformations or even fissures in the wood. Splitting can then occur either within the wood, at the adhesive bonds at the wood-resin interface, or at the cohesive bonds within the resin (Kim 1988). After several hydrolysis cycles run either on UF films or on particleboards, films show little modification, while particleboards are deeply damaged; the origin of this intense degradation is to be found in the movement of the wood particles and therefore in the bonded joint rupture (Dinwoodie 1977; Irle and Bolton 1991).

Each of the phases involved (resin, interface, wood) can thus clearly undergo some degradation (chemical for resin and interface, mechanical for interface and wood). Some methods have been developed to qualify these degradations (formaldehyde release, rupture strength), but they cannot account for all the phenomena occurring during hydrolytic degradation.

We tried, therefore, to quantify the deterioration of the bonded joint through measurement of a physical property whose variations with hydrolysis time represent a modification in the structure probably related to a decrease of mechanical characteristics. Permeability and diffusivity could both meet these specifications. Permeability is only characteristic of a geometric modification, whereas diffusivity can depend on chemical deterioration as far as the solute partition coefficient is usually connected with the chemical nature of the phases involved. Thus we chose to study the joint aging through the measurements of apparent diffusivity in the wood-UF resin joints.

MATERIALS AND METHODS

Materials

Our resin is a commercial product (PRESSAMINE 233 UF from NORSOLOR, Toulouse, France) whose ratio F/U is 1.3, resin solids content 64%, viscosity at 20°C 0.005 Pa.s, pH 8.4, and density 1.274. Our "standard adhesive mixture" was obtained by adding a hardener to that resin (1% mass of NH_4Cl with respect to the resin solids content).

The wood species is a softwood: grand fir (*Abies grandis*). This species was chosen for its gross structural simplicity, its relative homogeneity, and its wide rings. Wafers are thin 20- × 20-mm sections of about 250–260 μm thickness. Microtome cuts were made in spring wood (earlywood) using a REICHERT OME microtome, with respect to the fiber direction (tangential-longitudinal). These wafers were held at a moisture content between 4 and 5% in a desiccator with silica gel.

Preparation of the wood-urea-formaldehyde adhesive sample

The standard adhesive mixture was deposited between two wood wafers (20 × 20 mm) with fiber direction perpendicular to each other, placed between two smooth polytetrafluorethylene (PTFE) sheets (1 mm in thickness) whose role is to make the recovery of the sample easier (Fig. 1).

This system was left at room temperature for 5 min under a load of 1.7 kg, allowing some water and resin to begin to migrate into the

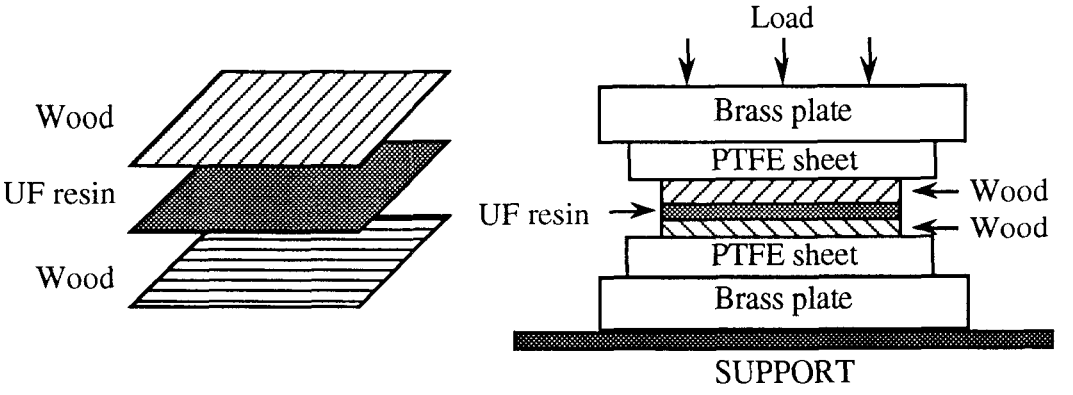

FIG. 1. Preparation of adhesive sample.

wood (prepressing). Then the system (PTFE sheets-sample) was kept between two brass plates preheated to 105°C and introduced into an oven at 105°C for 20 min under a load of 6.6 kg. Considering the dimensions of the wood sections and the load, the samples were under a pressure of about 0.16 MPa.

After separation of the PTFE sheets, the total thickness of the sample was measured with a micrometer (ROCH model 25).

Aging of adhesive samples

In order to shorten the duration of the experiments, aging of samples was not carried out in an isothermal gaseous phase with controlled moisture content, but by immersion in distilled water at room temperature (duration between 3 and 60 h). After each treatment, the samples were dried in a desiccator with silica gel (drying time: 5 days).

Most of our samples underwent three hydrolyses, the duration being chosen so that the same total hydrolysis time could be obtained after one, two, or three cycles. Table 1 summarizes the aging conditions of the eight samples tested.

Measuring apparent diffusivity

The diffusivity was measured in a classical Wicke and Kallenbach [1941] system, made from two low volume cells separated by the sample (Fig. 2).

The volumes of the two cells were $V_1 = 14.72 \times 10^{-6}$ m^3 and $V_2 = 13.58 \times 10^{-6}$ m^3, respectively. The gas distributor was made from a tube (⅛ in. OD) perforated with four openings 0.5 mm in diameter; the gas velocity at the outlet of these openings was high enough to reduce the stagnant zones inside the cell. The sample was glued onto its support with

TABLE 1. *Aging conditions of samples.*

Sample	First hydrolysis time (h)	Total immersion time (h)	Second hydrolysis time (h)	Total immersion time (h)	Third hydrolysis time (h)	Total immersion time (h)
N° 1	3	3	3	6	6	12
N° 2	6	6	6	12	6	18
N° 3	12	12	6	18	6	24
N° 4	18	18	6	24	12	36
N° 5	24	24	12	36	36	72
N° 6	36	36	12	48	24	72
N° 7	48	48	12	60	12	72
N° 8	60	60	12	72	—	—

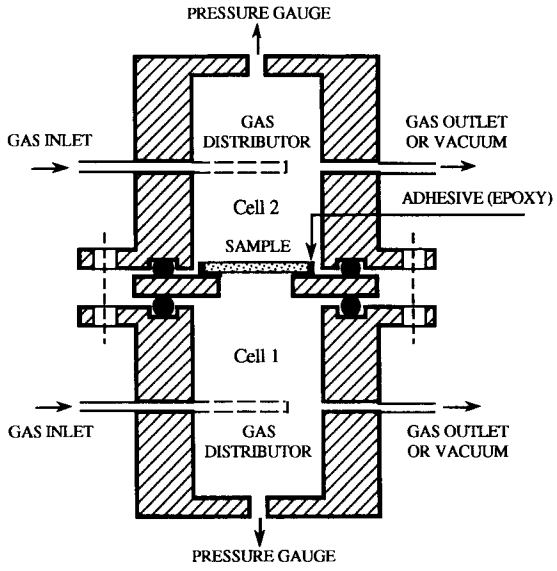

FIG. 2. Diffusion cell.

an epoxy adhesive, through which diffusion is very low, so that the solute transfer takes place primarily through the sample (see Fig. 2).

Both cells can be filled up or cleared using nitrogen or helium delivered from compressed gas bottles and flowing through a molecular sieve and silica gel in order to remove the remaining traces of impurities or water. The experimental apparatus is shown in Fig. 3.

Helium and nitrogen were analyzed with a gas chromatograph on a molecular sieve 5 Å (5 m in length, ¼″ in diameter); analytical conditions of the runs were: column temperature 100°C, detector (TCD) temperature 130°C, gas flow (nitrogen or helium) 30 mL/min. A previous calibration of the detector allowed determination of the gas concentrations.

Experiments were run with cells 1 and 2 closed. Cell 1 is cleared by helium, cell 2 by nitrogen. At zero time, both cells were closed; sampling at defined time allows determination of the helium and nitrogen concentration in

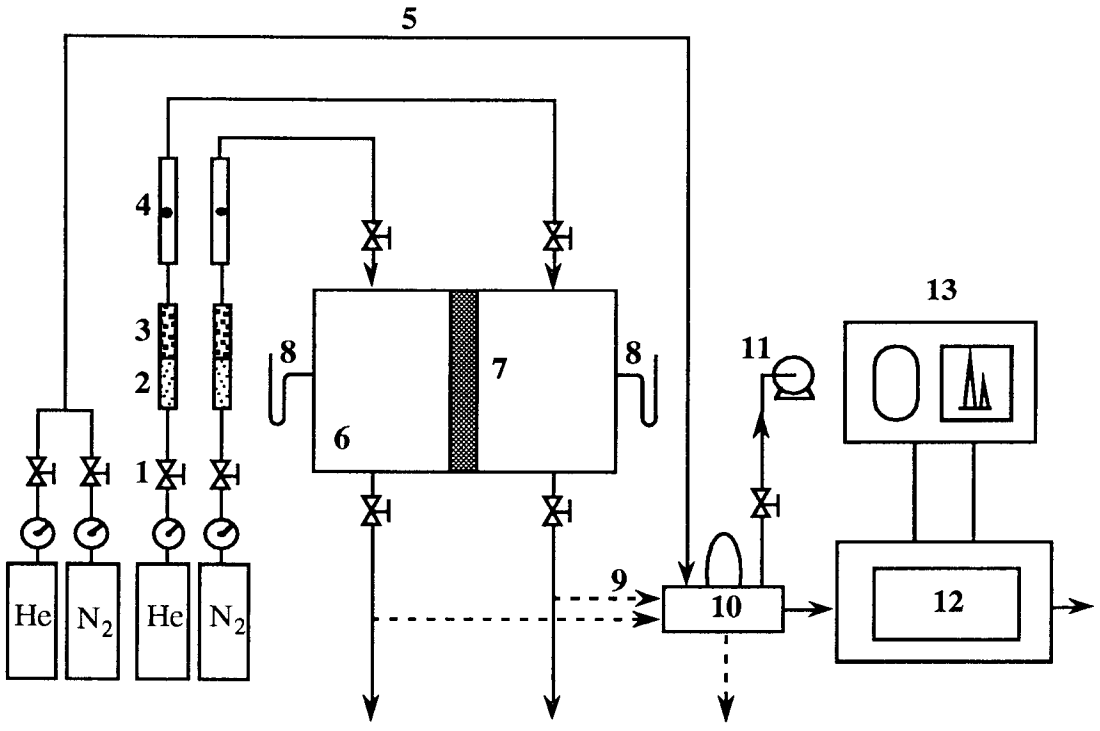

FIG. 3. Experimental apparatus. 1 = Needle valve; 2 = Molecular sieve; 3 = Silica gel; 4 = Flowmeter; 5 = Vector gas; 6 = Diffusion cell; 7 = Adhesive sample; 8 = Pressure gauge; 9 = Gas sampling; 10 = Injection system (sampling loop, 6 port-valve); 11 = Rotary vane vacuum pump; 12 = Gas chromatograph; 13 = Integrator.

each cell. In order to remove the effect of the sample volume (not negligible in comparison with the volumes of the cells), each experiment uses only one sample and is repeated to obtain the concentrations at different times.

MODELLING OF THE DIFFUSION EXPERIMENTS

Solute transfer analysis

Let C_{A1} and C_{A2} be the solute concentrations at time t in cells 1 and 2 and assume that the solute A transfer appears from cell 1 to cell 2. In the most general case, this transfer shows the following steps:

- a convective transfer between the fluid and the sample surface in cell 1, which is characterized by a transfer coefficient k_1.
- a partition of the solute at the sample surface between the gaseous and the solid phases, characterized by a partition coefficient m.
- a diffusional transfer of the solute throughout the sample, characterized by a diffusion coefficient D.
- a partition of the solute at the sample surface between the solid and the gaseous phases, characterized by a partition coefficient m.
- a convective transfer between the sample surface and the fluid in cell 2, which is characterized by a transfer coefficient k_2.

If the involved processes (transfer and partition) are assumed to be linear, the solute transfer from cell 1 to cell 2 can be characterized by a global coefficient K as follows:

$$\frac{1}{K} = \frac{1}{k_1} + \frac{me}{D} + \frac{1}{k_2} \tag{1}$$

In Eq. (1), e represents the sample thickness. For each time, the specific flow of transferred solute between both cells:

$$\Phi_A = K(C_{A1} - C_{A2}) \tag{2}$$

The transfer coefficient K is characteristic of the solute and the wood-resin sample, for the solute diffusivity in gaseous phase is generally much greater then the diffusivity in the solid phase. The transfer resistances $1/k_1$ and $1/k_2$ can be neglected before the internal resistance, and as a first approximation the coefficient K is expressed as:

$$K = \frac{D}{me} \tag{3}$$

The diffusivity D and the partition coefficient m depend on the solute nature and on the temperature, as will the transfer coefficient K. The procedure for preparing our samples leads to samples having approximately the same thickness; but K being directly dependent on e, we preferred to characterize the samples by the value e K which is named *apparent diffusivity* and quoted $\mathbb{D}$. A priori, $\mathbb{D}$ can depend on the type of transferred solute.

With this apparent diffusivity, the flow of solute A transfered from cell 1 to cell 2 is written as:

$$\Phi_A = \frac{\mathbb{D}_A}{e}(C_{A1} - C_{A2}) \tag{4}$$

Modeling of the diffusion cell (both cells being a closed system)

Both cells 1 and 2 being filled up at zero time with solute A (helium) or solute B (nitrogen), the mass balance equations at instant t are written as follows:

$$V_1\frac{dC_{A1}}{dt} + V_2\frac{dC_{A2}}{dt} = 0 \tag{5}$$

$$V_2\frac{dC_{A2}}{dt} = \frac{\mathbb{D}_A S}{e}(C_{A1} - C_{A2}) \tag{6}$$

under the initial conditions:

$$C_{A1} = C^0_{A1} \text{ and } C_{A2} = C^0_{A2} \tag{7}$$

In Eq. (6), S is the transfer area between the sample and the gaseous phases ($S = 1.77 \times 10^{-4}m^2$).

With relation (7), integration of Eq. (6) leads to:

$$-\ln\left[\frac{1 + \frac{V_1}{V_2}\frac{C^0_{A1}}{C^0_{A2}} - \frac{V_1 + V_2}{V_2}\frac{C_{A1}}{C^0_{A2}}}{1 - \frac{C^0_{A1}}{C^0_{A2}}}\right] =$$

$$= \frac{V_1 + V_2}{V_1 V_2} \frac{\mathbb{D}_A S}{e} t \qquad (8)$$

$$-\ln\left[\frac{1 + \frac{V_2}{V_1}\frac{C^0_{A2}}{C^0_{A1}} - \frac{V_1 + V_2}{V_1}\frac{C_{A2}}{C^0_{A1}}}{1 - \frac{C^0_{A2}}{C^0_{A1}}}\right] =$$

$$= \frac{V_1 + V_2}{V_1 V_2} \frac{\mathbb{D}_A S}{e} t \qquad (9)$$

These relations can be written in the same form for solute B; one has only to replace the subscript A by the subscript B.

Modelling hypothesis

The solute mass balances in the cells [Eqs. (5) and (6)] imply several hypotheses:

- Our system can be considered as globally isothermal. This hypothesis is verified, because our experiments are run at room temperature.
- The solute transfer within the sample does not alter it. Some authors (e.g., Blomquist and Olson 1957) reported a formaldehyde release when a gas (N_2, CO and CO_2) flowed over wood-resin products. That release was probably due to the moisture content of the gas. In fact, with wet gases, we detected during our experiments an interfering compound, which does not appear when the gas is dry. Our gases being dried and purified, we can assume that solute diffusion does not alter the sample.
- Both cells are at the same pressure. Under these conditions, the solute transfer in the sample occurs only by diffusion. During the experiments, we measured, using a differential pressure gauge, the pressure drop between cell 1 (helium) and cell 2 (nitrogen). Under our operating conditions, the pressure drop ΔP is not strictly equal to zero, but it remains less than 30 mm of water; as far as the apparent diffusivities seem not to depend on the system used, one can admit that this pressure drop affects neither the flow of transferred solute, nor the value of the apparent diffusivity.

RESULTS AND DISCUSSION

Diffusivity of an unaltered sample

As an example, Fig. 4 shows the results for an unaltered sample. Figure 4a shows the change of concentrations versus time for each solute (helium and nitrogen) in each cell (1 and 2), while Fig. 4b explains Eqs. (8) and (9).

From the straight lines in Fig. 4b, and including the values of cell volumes, sample area and thickness, one can determine the apparent diffusivity of the sample (Table 2).

These values of diffusivity are thus consistent; even if the helium diffusivity seems to be slightly greater ($\mathbb{D}_{He} = 5.41 \times 10^{-9}$ m$^2\cdot$s^{-1}; $\mathbb{D}_{N2} = 5.15 \times 10^{-9}$ m$^2\cdot$s^{-1}), the mean value ($\mathbb{D} = 5.3 \times 10^{-9}$ m$^2\cdot$s^{-1}) can be assumed to be representative of the sample for both inert solutes considered.

This value is greater than those given in the literature for diffusion in polymers (from 10^{-15} to 10^{-11} m$^2\cdot$s^{-1} [Van Krevelen 1976]).

With the assumption of porous structure of the sample being made up from cylindrical pores with a mean diameter d, the diffusional transfer within the pores depends on the Knudsen number (Kn = d/λ where λ is the mean free path of gas molecules). But apparent diffusivities being much smaller than Fick's molecular diffusion coefficients for helium and nitrogen, if the sample is effectively porous, the diffusion will be of Knudsen type. Under these conditions, the diffusion coefficient is linked to the mean pore diameter through the relation:

$$\mathbb{D}_K = \frac{1}{3} d \sqrt{\frac{8RT}{\pi M}} =$$

$$= 1.534 d \sqrt{\frac{T}{M}} \quad \text{(SI units)} \qquad (10)$$

Identifying our diffusivities ($\mathbb{D}_{He} = 5.41 \times 10^{-9}$ m$^2\cdot$s^{-1}; $\mathbb{D}_{N2} = 5.15 \times 10^{-9}$ m$^2\cdot$s^{-1}) to the

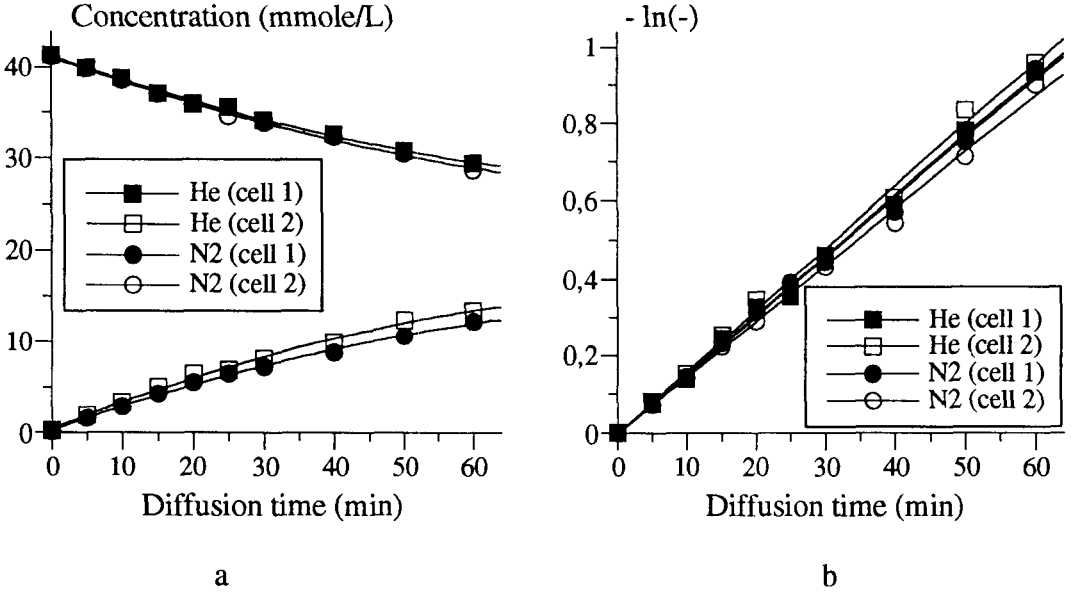

FIG. 4. Experimental results for an unaltered sample. 4a) Concentrations vs. time; 4b) Calculation from Eqs. (8) and (9).

Knudsen diffusion coefficients leads to the following values of mean pore diameter:

$$d = 0.130 \times 10^{-10} \text{ m for helium}$$
$$d = 0.328 \times 10^{-10} \text{ m for nitrogen.}$$

These values are smaller than the molecular radii of helium ($\sigma_{He} = 2.70 \times 10^{-10}$ m) and nitrogen ($\sigma_{N2} = 3.681 \times 10^{-10}$ m) molecules. Consequently, one can state that the resin in the sample does not have a porous structure and that the solute transfer is really carried out through a diffusional mechanism within the solid phase.

Our apparent diffusivity values seem to be higher than those found in the literature, but they depend on the thickness e that we assumed to be equal to the total thickness of the sample. As a matter of fact, the diffusional thickness in the resin is much lower, and as a consequence, the measured values can be consistent with those of the literature.

It is of some interest to point out that these diffusivities remain much lower than the diffusivity of gases in wood in the tangential direction (from 10^{-8} to 10^{-5} $m^2 \cdot s^{-1}$ [Siau 1971]).

TABLE 2. *Apparent diffusivities for an unaltered sample.*

	Helium		Nitrogen	
	Cell 1	Cell 2	Cell 1	Cell 2
Apparent diffusivity $\mathbb{D}$ (10^{-9} $m^2 \cdot s^{-1}$)	5.33	5.50	5.30	5.00

Hydrolytic degradation of samples

In order to decrease the diffusion time and the duration of experiments, the following diffusivity measurements were carried out on eight samples (Table 1) of the same thickness, but with reduced UF resin mass (Table 3) in comparison with those discussed in the previous section. Table 3 also summarizes the conditions for preparing the samples and the initial apparent diffusivities, determined from the variation of the helium concentration in both cells.

The diffusivities measured on samples before and after degradation through immersion

TABLE 3. *Preparation of samples and initial apparent diffusivities.*

Sample	Wood cuts		Mass of glue (mg)	Produced sample		Apparent diffusity D_{He} (10^{-8} m^2·s^{-1})
	Thickness (μm)	Mass (mg)		Thickness (μm)	Mass (mg)	
N° 1	260	23	62	490	87	2.75
	260	25				2.84
N° 2	260	23	62	495	81	2.31
	260	24				2.44
N° 3	260	25	61	490	85	2.48
	260	23				2.52
N° 4	260	27	63	500	85	2.05
	260	24				2.21
N° 5	260	26	63	490	85	2.49
	260	23				2.54
N° 6	260	26	62	495	85	2.33
	260	23				2.38
N° 7	260	27	61	490	83	2.71
	260	22				2.84
N° 8	260	24	63	495	88	2.59
	260	27				2.64

in water and drying are reported in Table 4 for different immersion times and after 1, 2, or 3 hydrolysis cycles. Times given in this table are total immersion times.

Because the initial apparent diffusivities are different, it is difficult to compare the absolute values of the diffusivities. Thus we will represent the effect of degradation as the relative variation of diffusivity, that is:

$$\frac{\Delta\mathbb{D}}{\mathbb{D}} = \frac{\mathbb{D}_t - \mathbb{D}_0}{\mathbb{D}_0} \qquad (11)$$

where $\mathbb{D}_o$ and $\mathbb{D}_t$ represent the apparent dif-

TABLE 4. *Apparent diffusivities of samples before and after aging.*

Sample	Cell	Apparent diffusivity D_{He} (10^{-8} m^2·s^{-1}) vs time									
		0 h	3 h	6 h	12 h	18 h	24 h	36 h	48 h	60 h	72 h
N° 1	C_1	2.75	3.09	3.78	4.48						
	C_2	2.84	3.27	4.11	4.81						
N° 2	C_1	2.31		2.53	3.22	3.77					
	C_2	2.44		2.77	3.72	4.23					
N° 3	C_1	2.48			3.04	3.89	4.10				
	C_2	2.52			3.21	4.13	4.35				
N° 4	C_1	2.05				2.53	3.40	3.51			
	C_2	2.21				3.02	3.84	4.04			
N° 5	C_1	2.49					3.45	4.00	4.23		
	C_2	2.54					3.73	4.46	4.58		
N° 6	C_1	2.33						3.49	3.87		3.74
	C_2	2.38						3.79	4.21		4.19
N° 7	C_1	2.71							3.98	4.44	4.41
	C_2	2.84							4.41	4.88	4.89
N° 8	C_1	2.59								4.18	4.27
	C_2	2.64								4.42	4.61

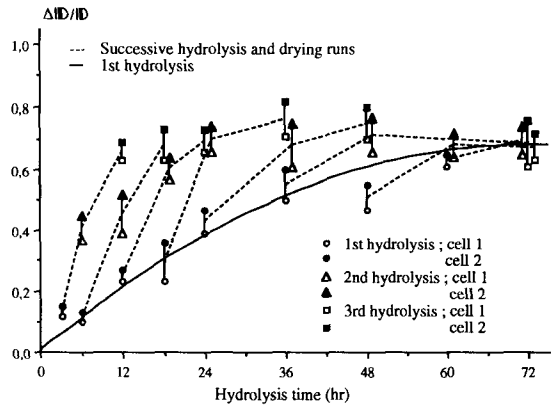

FIG. 5. Relative variation of apparent diffusivity of samples after hydrolysis.

fusivities of the sample unaltered and after an immersion time t respectively. Experimental values of $\Delta\mathbb{D}/\mathbb{D}$ versus total hydrolysis time are pointed out in Fig. 5.

Looking at Fig. 5, one can make several remarks:

- The relative variation of diffusivity increases with the immersion time for the first degradation.
- For the same immersion time, sample degradation is more pronounced for multi-steps than for only one-step experiments. Thus the sample is undergoing some sort of degradation during drying.
- After 1 or 2 drying cycles, the influence of immersion time on the relative variation of diffusivity becomes less.

The relative diffusivity variations show an asymptotic trend, but we could not totally verify this point because during immersion and drying the samples ended up splitting. For this reason, we could not obtain unsplit samples after 60–72-h immersion time.

This apparent diffusivity variation during three successive hydrolysis cycles indicates the degradation of the sample. In order to clarify the chemical and/or mechanical aspects of this degradation, we studied the evolution of the aqueous solution in which the hydrolysis took place. As a matter of fact, absorbed water favors the hydrolysis of the UF adhesive and also leads to the release of the resin acids. This acidity plays an important role in resin hydrolysis. Thus we studied the variations of pH in the aqueous solution due to the release of acids during the hydrolysis cycles.

The variations of pH were measured with a Metrohm AG CH-9100 pHmeter with a glass electrode in an isothermal closed system. The apparatus is calibrated with known buffer solutions. The hardened UF resin (as powder less than 100 μm in diameter) or the bonded sample (as 500 μm-thick film) is immersed in distilled water with initial pH being between 5.5 and 5.7. The mass ratio resin or sample to water has been held at 1/30. Hydrolysis time was 20 h; after each cycle, the solid was dried (desiccator) before undergoing another possible hydrolysis cycle.

Figure 6a shows the results of experiments run on resin particles, which were hydrolyzed three times and dried after each hydrolysis cycle. One can note that the pH variation due to the release of the resin acids is very large at the beginning of the first hydrolysis cycle and that this variation decreases markedly after each hydrolysis cycle, so that it is almost insignificant after the third hydrolysis cycle.

Similar hydrolysis cycles were run on bonded wood samples (Fig. 6b). The variation of pH is smaller than the one observed with the resin alone, because of the lower quantity of resin in the sample. Nevertheless the pH variation decreases with the number of hydrolysis cycles.

Finally, the observed variation of pH takes place mainly during the first hydrolysis cycle. The effect of the second hydrolysis cycle can still be observed, but the third one can be considered as negligible. Finally the drying step seems not to activate any acid release, judging only from the acidity of the medium.

Figure 5 showed that degradation was going on during the second and third hydrolysis; hence it appears that the main part of the chemical degradation of the sample takes place during the first hydrolysis, while the mechan-

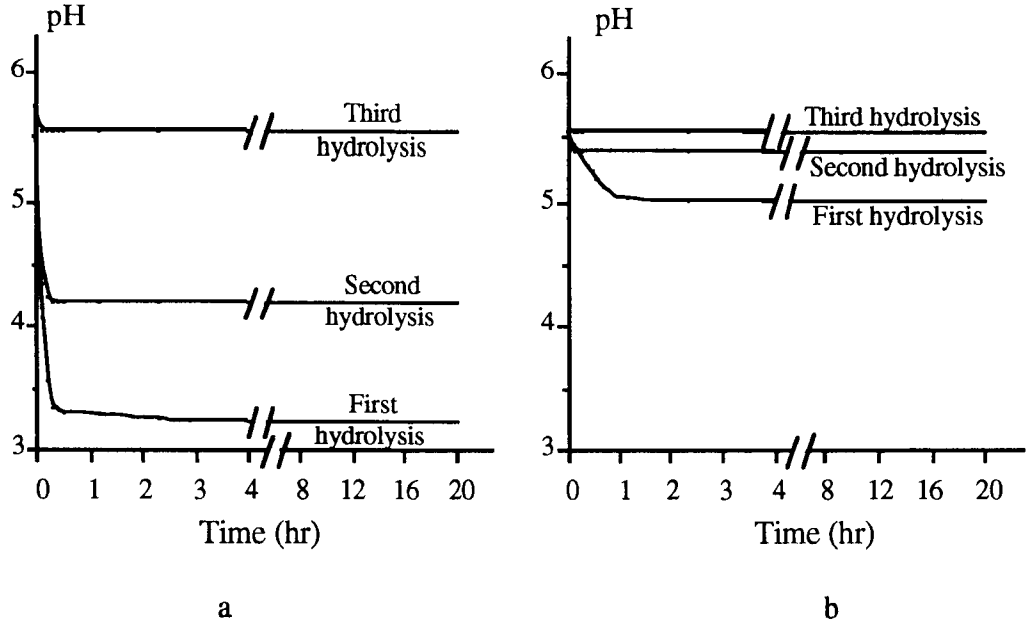

FIG. 6. Variation of pH during hydrolysis cycles. 6a) hydrolysis of UF resin; 6b) hydrolysis of adhesive sample.

ical degradation continues during the following cycles.

CONCLUSION

We can thus quantify the aging of an adhesive joint by the measurement of apparent diffusivities of two inert solutes through the joint. This measurement is of interest because it includes the partition coefficients of the solutes between phases and then both mechanical and chemical structure modifications.

Diffusivity increases with immersion time to an asymptotic value; our values show that the resin does not have a porous structure and that the solute transfer is effectively carried out by a diffusional mechanism within the solid phase. Moreover, the joint degradation is greater, for the same total time, when undergoing several immersion-drying cycles rather than just one. Finally, the acidity measurements show that during cyclic hydrolysis the chemical degradation of the joint takes place mostly during the first hydrolysis, while mechanical degradation continues during the next cycles; this point confirms that part of the degradation has a mechanical origin.

REFERENCES

BLOMQUIST, R. F., AND W. Z. OLSON. 1957. Durability of urea-resin glues at elevated temperatures. Forest Prod. J. 7:266–272.

DINWOODIE, J. M. 1977. Causes of deterioration of UF chipboard under cyclic humidity conditions—I. Performances of UF adhesive films. Holzforschung 31:51–55.

IRLE, M. A., AND A. J. BOLTON. 1991. Physical aspects of wood adhesive bond formation with formaldehyde based adhesive. III. The creep behavior of formaldehyde based resins at different relative humidities. Holzforschung 45:69–73.

KIM, J. S. 1988. Urea-formaldehyde and melamine resins. Daekwang Press, Seoul, and Tokyo. 572 pp.

MYERS, G. E. 1982. Hydrolytic stability of cured urea-formaldehyde resins. Wood Sci. 15:127–138.

———. 1990. Formaldehyde liberation and cure behavior of urea-formaldehyde resins. Holzforschung 44:117–126.

SIAU, J. F. 1971. Flow in wood. Syracuse University Press, Syracuse, NY. 131 pp.

TROUGHTON, G. E., AND S. Z. CHOW. 1975. Effect of fortifier addition on the curing reactions of urea-formaldehyde adhesives. Holzforschung 29:214–217.

APPLICATION OF THE LIFSHITZ-VAN DER WAALS ACID-BASE APPROACH TO DETERMINE WOOD SURFACE TENSION COMPONENTS

Douglas J. Gardner

Associate Professor of Wood Science
Institute of Wood Research
Michigan Technological University
Houghton, MI 49931-1295

(Received January 1996)

ABSTRACT

Improvements are being made in the fundamental descriptions of surface thermodynamics, and it is important to apply these new concepts to wood. The purpose of this paper is to determine wood surface tension components using the Lifshitz-van der Waals/acid-base approach. Zisman plot, geometric-mean, and harmonic-mean wood surface tension determinations are also made for comparative purposes. Lifshitz-van der Waal forces appear to account for the majority of wood surface tension, and the acid-base character comes primarily from the electron donating γ-sites. The contribution of γ-sites on the wood surface to fundamental wood-adhesive interactions may have considerable implications in the gluing and finishing technology of wood, and it deserves further study. The Lifshitz-van der Waals/acid-base approach provides for greater accuracy in calculating wood surface tension components than the geometric-mean and harmonic-mean equations because it is based on the contribution of contact angles from five liquids versus two liquids. In some instances, the critical surface tension of wood obtained using Zisman plots compares favorably with the total surface tension obtained by the Lifshitz-van der Waals/acid-base approach.

Keywords: Wood, surface tension, contact angle, Lifshitz-van der Waals/acid-base, pH.

INTRODUCTION

New techniques and approaches to studying fundamental aspects of surface chemistry are being applied to wood with good success (Gardner et al. 1996). In particular, instrumental analysis techniques like inverse gas chromatography (Kamdem et al. 1993), dynamic contact angle analysis (Gardner et al. 1991), atomic force microscopy (Hanley and Gray 1994), and X-ray photoelectron spectroscopy (Dorris and Gray 1978) have provided an improved understanding of the chemical and physical characteristics of the wood surface. Along with the newer instrumental techniques, improvements have been made in the fundamental descriptions of surface thermodynamics (van Oss et al. 1988; Liu et al. 1995; Wu et al. 1995). However, some recent research describing wood surface thermodynamics used approaches developed 30 to 40 years ago, including Zisman's critical surface tension determinations and Good-Girifalco surface energy calculations (Gardner et al. 1991; Liptakova and Kudela 1994). The Good-Girifalco approach of separating surface energy into polar and nonpolar (dispersive) components still remains a forefront topic in surface and colloid science (Etzler and Conners 1995), so it is not surprising to find its current application in wood science. However, it is important to apply the new fundamental descriptions of surface thermodynamics to wood.

OBJECTIVE

It is the purpose of this paper to determine wood surface tension components using the Lifshitz-van der Waals/acid-base approach (van Oss et al. 1988). Zisman plot, geometric mean, and harmonic-mean wood surface tension determinations will also be made for comparative purposes.

Wood and Fiber Science, 28(4), 1996, pp. 422–428

THEORETICAL BACKGROUND

Thomas Young, in 1805, first described the equation that determines the interaction of a liquid drop with a solid surface.

$$\gamma_S - \gamma_{SL} = \gamma_L \cos\Theta \quad (1)$$

where γ is the surface free energy (surface tension), the subscripts S, SL, and L refer to the solid, solid-liquid, and liquid surface tensions respectively, and θ is the contact angle. Girifalco and Good (1957) derived a relationship for γ_{SL} that assumed only intermolecular force interactions were important in determining surface tension components between a liquid and a solid.

$$\gamma_{SL} = \gamma_S + \gamma_L - 2(\gamma_S\gamma_L)^{1/2} \quad (2)$$

Furthermore, the total surface free energy γ_T is divided into polar and nonpolar (dispersive) components. Thus

$$\gamma_T = \gamma^d + \gamma^p \quad (3)$$

where γ^d surface free energy resulting from London dispersion forces. London forces result from the polarizability of electron orbitals and are common to all intermolecular interactions. The term γ^p is the surface free energy resulting from dipole-dipole, induced dipole, and hydrogen bonding interactions. Expanding the Good-Girifalco equation

$$\gamma_{SL} = \gamma_S + \gamma_L - 2(\gamma_S^d\gamma_L^d)^{1/2} - 2(\gamma_S^p\gamma_L^p)^{1/2} \quad (4)$$

The Good-Girifalco (geometric-mean) equation can be combined with the Young equation to calculate contact angles

$$(1 + \cos\theta)\gamma_L = 2(\gamma_S^d\gamma_L^d)^{1/2} + 2(\gamma_S^p\gamma_L^p)^{1/2} \quad (5)$$

Fowkes (1974) and more recently van Oss et al. (1988) have suggested separation of the polar components into separate Lewis acid (+) and Lewis base (−) terms. Thus

$$\gamma^p = 2(\gamma^+\gamma^-)^{1/2} \quad (6)$$

Van Oss et al. (1988) also offered a more rigorous derivation of nonpolar surface energy components based on Lifshitz-van der Waals interactions γ^{LW} (where γ^d is approximately equivalent to γ^{LW}). By accounting for Lewis acid-base interactions and Lifshitz-van der Waals interactions, the Young-Good-Girifalco-Fowkes equation becomes

$$(1 + \cos\theta)\gamma_L = 2[\gamma_S^{LW}\gamma_L^{LW})^{1/2} + (\gamma_S^+\gamma_L^-)^{1/2} + (\gamma_L^-\gamma_L^+)^{1/2}] \quad (7)$$

By using nonpolar liquid probes (total γ^{LW}), and polar liquid probes with known electron-acceptor γ^+ (acid) and electron-donor γ^- (base) parameters, the solid surface energy components γ^{LW}, γ^+, and γ^- can be determined using contact angle measurements.

METHODS AND MATERIALS

Contact angle measurements

Dynamic contact angle (DCA) measurements were made with a Cahn Instruments DCA 322 on wood veneer samples following the procedures described by Gardner et al. (1991). The sliced wood veneers were obtained from a local manufacturer. The veneers were commercially dried on a screen dryer with gas-fired jets. Feed temperature of the dryer was 79.4°C and outlet temperature was 110°C. Veneer drying time averaged eight minutes. After the veneers were received from the local producer, they were conditioned to 8% moisture content at 22°C. The species examined were heartwood of ash (*Fraxinus americana* L.), cherry (*Prunus serotina* Ehrh.), hard maple (*Acer saccharum* Marsh.), red oak (*Quercus rubra* L.), white oak (*Quercus* spp.), and walnut (*Juglans nigra* L.). Samples (25 × 25 × 0.7 mm) were sanded with 220 grit sandpaper to provide a fresh surface, and end-coated prior to DCA measurements parallel to the veneer grain. Testing speed for the DCA measurements was 194 microns/s. The contact angle probe liquids, and values of the surface tension components and parameters are found in Table 1. All contact angle probe liquids were either reagent or HPLC grade. For each species, ten contact angles were collected per probe liquid and were averaged for calculation of surface tension components. The contact angle

TABLE 1. *Values of the surface tension components and parameters (in mJ/M²) of probe liquids used for contact angle measurements at 20°C.*[a]

Liquids	γ_L(mJ/M²)	γ^{LW}(mJ/M²)	γ^{AB}(mJ/M²)	γ^+(mJ/M²)	γ^-(mJ/M²)
α-Bromonapthalene	44.4	44.4	≈0	≈0	≈0
Ethylene glycol	48	29	19	≈1.92	≈47.0
Formamide	58	39	19	2.28	39.6
Glycerol	64	34	30	3.92	57.4
Water	72.8	21.8	51	25.5	25.5

[a] From Wu et al. (1995).

averages and standard deviations for each species and probe liquid are shown in Table 2.

Calculation of surface tension components

Determination of the solid surface energy components γ^{LW}, γ^+, and γ^- for the wood samples were calculated using Eq. 7. Because the contact angle, liquid surface tension, and liquid surface energy components are known, the solid surface energy components can be calculated using a set of simultaneous equations. In this instance, a set of five simultaneous equations representing the five probe liquids were used to calculate the three unknown wood surface energy components. The simultaneous equations were solved using a least-square routine in QuattroPro® (spreadsheet).

For comparative purposes, Eq. 5 (geometric-mean) and the harmonic-mean equation (8) were used to calculate surface tension components using the two-liquid method. Water contact angle data were used with contact angle data from the following probe liquids: α-bromonapthalene (α-brom.), ethylene glycol (E.G.), formamide (form.), and glycerol (gly.) to calculate the geometric-mean and harmonic-mean surface tension components. The harmonic-mean equation proposed by WU (1971)

$$\gamma_{LV}(1 + \cos\Theta) = \frac{4\gamma_S^d\gamma_L^d}{\gamma_S^d + \gamma_L^d} + \frac{4\gamma_S^p\gamma_L^p}{\gamma_S^p + \gamma_L^p} \quad (8)$$

is based on an empirical approach to calculating surface tension parameters and is considered to be more suitable than the geometric-mean in calculating the polar component of polymeric surfaces. Both the geometric-mean and harmonic-mean method have been used in calculating the surface tension components of wood (Nguyen and Johns 1978). Critical surface tension γ_c values were also determined by Zisman plots (Zisman 1964) using the probe liquids in Table 1. Calculations for determining the geometric-mean, harmonic-mean, and Zisman surface tension values are available in the Cahn DCA Applications Software (1991).

pH measurements

The determination of pH for the wood samples was made using the methods described by Moore and Johnson (1985). One part by weight of freshly ground (to pass 40-mesh screen) par-

TABLE 2. *Average advancing contact angles of the probe liquids used in this study.*

Species	Probe liquid (average contact angle and standard deviation)				
	α-bromonapthalene	Ethylene glycol	Formamide	Glycerol	Water
Ash	9.79 (2.38)	17.47 (7.73)	0 (0)	59.82 (8.91)	23.66 (9.97)
Cherry	0 (0)	13.95 (5.21)	0 (0)	50.29 (10.73)	44.39 (5.23)
Maple	0 (0)	14.26 (4.54)	0 (0)	48.37 (2.05)	34.91 (7.06)
Red oak	0 (0)	16.23 (4.89)	28.52 (4.74)	55.96 (5.04)	40.11 (2.74)
White oak	20.38 (6.06)	55.48 (5.86)	33.13 (9.09)	58.49 (3.02)	59.56 (9.43)
Walnut	14.3 (5.72)	36.12 (5.85)	32.91 (10.53)	43.42 (10.96)	26.33 (12.88)

ticles was placed in three parts of freshly boiled and cooled distilled water. The sample and water were mixed until the particles were wet, and the pH was measured with a glass electrode pH meter after 5 min.

RESULTS

Lifshitz-van der Waals/acid-base approach

The surface tension components determined using the Lifshitz-van der Waals/acid-base approach are shown in Table 3. The total surface energy varied from 40 mJ/M^2 for white oak to 54.3 mJ/M^2 for cherry. Lifshitz-van der Waal forces appear to account for the majority of wood surface tension with values ranging from 34.02 mJ/M^2 for white oak to 47.46 mJ/M^2 for cherry. Acid-base contribution varied from 0.6 mJ/M^2 for ash to 8.3 mJ/M^2 for red oak. It is important to note that the majority of acid-base character comes from the electron donating γ^- sites on the wood surface. At first glance, this electron donating behavior goes against conventional wisdom because wood exhibits a slightly acidic pH (Table 3). However, it should be pointed out that pH measurements are made on the bulk wood, and contact angles are based on surface sensitive measurements. It is well established that extractives dominate wood surface thermodynamic behavior (Gardner et al. 1996). Many of the extractives present in the species evaluated contain aromatic compounds (Rowe and Conner 1979), and aromatic rings are considered soft bases (electron donating) (March 1977). Therefore, it is not unusual that the surface character of wood is primarily basic or monopolar in nature. In fact, many synthetic and biopolymer materials appear to have to γ^- monopolar surfaces (van Oss et al. 1987).

Zisman plots

The critical surface tension values for the wood species are shown in Table 3. Critical surface tension values varied from 10.8 mJ/M^2 for walnut to 48.1 mJ/M^2 for cherry. The critical surface tension values for red oak and ash compared quite favorably with the surface tension values calculated using Eq. 7. However, the critical surface tension value obtained for walnut is unreasonably low. It is well known that the choice of probe liquids used to measure critical surface tensions can have an effect on the values obtained (Zisman 1977). It should be pointed out that the probes used in this study were chosen for calculating acid-base character, and they may not be the best choice for determining wood critical surface tensions. Earlier studies have shown that water-ethanol and water-acetic acid solutions are good probes for determining critical surface tensions on wood (Gardner et al. 1991; Gunnells 1992).

Geometric-mean and harmonic-mean approach

The wood surface tension components obtained by solving the geometric-mean and harmonic-mean equations are shown in Table 4. The γ_s values obtained by the geometric-mean equation were generally greater than the γ_s values obtained by the harmonic-mean equation. Nguyen and Johns (1978) favored the use of the harmonic mean-mean model for characterizing the wood surface thermodynamics. Depending on the two liquids used, γ_s calcu-

TABLE 3. *Surface tension components and parameters obtained by solving Eq. 7, and critical surface tension γ_c, values obtained by Zisman plots.*

Species	γ_c(mJ/M^2)	γ_s^{TOT}(mJ/M^2)	γ_s^{LW}(mJ/M^2)	γ_s^{AB}(mJ/M^2)	γ_s^+(mJ/M^2)	γ_s^-(mJ/M^2)	pH
Ash	42.9	43.23	42.63	0.6	0.001	67.35	5.9
Cherry	48.1	54.3	47.46	6.84	0.42	28.00	4.36
Maple	46.8	53.3	45.48	7.85	0.46	33.19	5.3
Red oak	46.8	47.97	39.67	8.30	0.46	37.74	4.67
White oak	31.4	40.0	34.02	5.98	0.39	22.80	4.32
Walnut	10.8	42.55	37.92	4.63	0.09	58.93	4.71

TABLE 4. *Surface tension components and parameters of wood obtained by solving the geometric-mean and harmonic-mean equations.*

Species	Probes*	Geometric-mean			Harmonic-mean		
		γ_s(mJ/M^2)	γ_s^d(mJ/M^2)	γ_s^p(mJ/M^2)	γ_s(mJ/M^2)	γ_s^d(mJ/M^2)	γ_s^p(mJ/M^2)
Ash	Water-α-Brom	76.91	45.62	31.29	45.64	45.64	0
	Water-E.G.	87.84	2.68	85.16	74.02	13.87	60.15
	Water-Form.	71.52	20.63	50.89	71.45	24.31	47.14
	Water-Gly.	79.52	0.55	78.97	63.11	11.99	51.12
Cherry	Water-α-Brom	64.24	46.10	18.14	46.13	46.13	0
	Water-E.G.	54.29	16.19	38.1	55.19	20.09	35.1
	Water-Form.	62.73	42.0	20.73	63.11	35.6	27.51
	Water-Gly.	65.4	3.39	61.51	55.11	18.09	37.02
Maple	Water-α-Brom	69.12	47.06	22.06	47.12	47.12	0
	Water-E.G.	64.84	8.77	56.07	61.06	20.13	40.93
	Water-Form.	63.19	33.83	29.36	64.22	31.01	33.21
	Water-Gly.	66.2	4.67	61.53	59.59	15.98	43.61
Red oak	Water-α-Brom	67.0	46.98	20.02	47.05	47.05	0
	Water-E.G.	52.6	10.4	42.2	51.91	16.87	35.04
	Water-Form.	59.8	30.6	29.2	60.87	25.24	35.63
	Water-Gly.	66.7	2.77	63.93	58.34	14.21	44.13
White oak	Water-α-Brom	54.84	43.64	11.2	43.71	43.71	0
	Water-E.G.	46.94	5.29	41.65	46.9	8.59	38.31
	Water-Form.	50.85	35.33	15.52	50.92	29.25	21.67
	Water-Gly.	40.64	14.13	26.51	43.43	17.59	25.84
Walnut	Water-α-Brom	71.46	44.51	26.95	44.59	44.59	0
	Water-E.G.	87.42	1.28	86.14	70.35	10.07	40.93
	Water-Form.	63.19	12.03	54.52	65.35	16.95	33.21
	Water-Gly.	56.08	4.89	51.91	55.11	18.09	37.02

* Refer to text for abbreviations.

lated using the geometric-mean equation varied from 40.64 mJ/M^2 for white oak (water-glycerol) to 87.84 mJ/M^2 for ash (water-ethylene glycol). The γ_s calculated using the harmonic-mean equation varied from 43.43 mJ/M^2 for white oak (water glycerol) to 74.02 mJ/M^2 for ash (water-ethylene glycol). For a few liquid combinations, the harmonic-mean γ_s values were closer to the γ_s values obtained using the Lifshitz-van der Waals/acid-base approach (Table 3). However, there was no consistent trend among the γ_s values obtained using the three different methods of calculation.

DISCUSSION

The Lifshitz-van der Waals/acid-base approach provides for greater accuracy in calculating wood surface tension components than the geometric-mean and harmonic-mean equations because it is based on the contribution of contact angles from five liquids versus two liquids. Also, the fact that the acid-base character of the solid is obtained using Eq. 7 is a marked improvement over the geometric-mean and harmonic-mean calculations. As a *caveat,* it should be noted that there are some deficiencies in the use of acid/base measurements. There are no acid or base probe liquids with 100 percent acid or base character. Thus, different results could be obtained by use of different probe liquids. Future research should address this problem.

Any of the γ_s values obtained using the geometric-mean and harmonic-mean equations greater than 73 mJ/M^2 are unreasonably high. The γ_s values are larger than the surface tension of water, and are much greater than wood surface tension values reported in the literature. The thermodynamic nature of the chem-

ical components (extractives) comprising the wood surface would prohibit surface tension values greater than 73 mJ/M^2.

As mentioned earlier, the determination of critical surface tension values for wood are dependent on the choice of probe liquids. In some instances, the critical surface tension of wood obtained using Zisman plots compared favorably with the total surface tension obtained by the Lifshitz-van der Waals/acid-base approach. Therefore, the Zisman approach can still be considered a useful method for determining the total surface tension of wood. From the practical standpoint, knowing the total surface tension of wood is useful for understanding how an adhesive or finish will wet the wood. Perhaps more important, however, is understanding how the acid-base (i.e. electron donating) character of the wood surface will influence adhesive curing mechanisms. The contribution of the γ^- wood surface to fundamental wood-adhesive interactions may have considerable implications in the gluing and finishing technology of wood, and deserves further study.

CONCLUSIONS

The Lifshitz-van der Waals/acid-base approach to determine solid surface tension components was successfully applied to wood. Lifshitz-van der Waal forces appear to account for the majority of wood surface tension, and the acid-base character primarily comes from the electron donating γ^- sites. The Lifshitz-van der Waals/acid-base approach provides for greater accuracy in calculating wood surface tension components than the geometric-mean and harmonic-mean equations because it is based on the contribution of contact angles from five liquids versus two liquids. In some instances, the critical surface tension of wood obtained using Zisman plots compares favorably with the total surface tension obtained by the Lifshitz-van der Waals/acid-base approach. Therefore, the Zisman approach can still be considered a useful method for determining the total surface tension of wood.

ACKNOWLEDGMENTS

The author thanks Northern Michigan Veneer, Inc., Gladstone, MI, for providing the wood veneer, and Daniel Mahler for collecting the surface tension data used in this study. Dr. C. J. van Oss provided helpful comments on the nature of monopolar surfaces. Funding for this research was provided by the Institute of Wood Research at Michigan Technological University.

REFERENCES

CAHN. 1991. CAHN DCA Applications Software. ATI Analytical Technology Inc., Madison, WI.

DORRIS, G. M., AND D. G. GRAY. 1978. The surface analysis of paper and wood fibers by ESCA (Electron Spectroscopy for Chemical Analysis). I. Application to cellulose and lignin. Cellulose Chem. Technol. 12:9–23.

ETZLER, F. M., AND J. J. CONNERS. 1995. The surface chemistry of paper: Its relationship to printability and other paper technologies. *In* T. E. Conners and S. Banergee, eds. Surface analysis of paper. CRC Press, Boca Raton, FL.

FOWKES, F. M. 1972. Donor-acceptor interactions at interfaces. J. Adhesion 4:155–159.

GARDNER, D. J., N. C. GENERALLA, D. W. GUNNELLS, AND M. P. WOLCOTT. 1991. Dynamic wettability of wood. Langmuir 7(11):2498–2502.

———, M. P. WOLCOTT, L. WILSON, Y. HUANG, AND M. CARPENTER. 1996. Our understanding of wood chemistry in 1995. Pages 29–36 *in* Proc. No. 7296 1995 Wood Adhesive Symposium, Forest Products Society.

GIRIFALCO, L. A., AND R. J. GOOD. 1957. A theory for the estimation of surface and interfacial energies. I. Derivation and application to interfacial tension. J. Phys. Chem. 61:904.

GUNNELLS, D. W. 1992. Utilizing DCA analysis to investigate the effects of environmental conditions on the surface of wood. Master's thesis, West Virginia University, Morgantown, WV.

HANLEY, S. J., AND D. G. GRAY. 1994. Atomic force microscope images of black spruce wood sections and pulp fibers. Holzforschung 48:29–34.

KAMDEM, D. P., S. K. BOSE, AND P. LUNER. 1993. Inverse gas chromatography characterization of birch wood meal. Langmuir 9(11):3039–3044.

LIPTAKOVA, E., AND J. KUDELA. 1994. Analysis of the wood-wetting process. Holzforschung 48:139–144.

LIU, F. P., D. J. GARDNER, AND M. P. WOLCOTT. 1995. A model for the description of polymer surface dynamic behavior. I. Contact angle vs. polymer surface properties. Langmuir 11(7):2674–2681.

MARCH, J. 1977. Advanced organic chemistry reactions, mechanisms, and structure. 2nd ed. McGraw Hill Book Co., New York, NY. P. 238.

MOORE, W. E., AND D. B. JOHNSON. 1985. Procedures for chemical analysis of wood and wood products. USDA Forest Serv. Forest Prod. Lab., Madison, WI.

NGUYEN, T., AND W.E. JOHNS. 1978. Polar and dispersion force contributions to the total surface free energy of wood. Wood Sci. Technol. 12:63–74.

ROWE, J.W., AND A.H. CONNER. 1979. Extractives in eastern hardwoods—A review. USDA Forest Serv. Gen. Tech. Rep. FPL-18. USDA Forest Prod. Lab., Madison, WI.

VAN OSS, C. J., M. K. CHAUDHURY, AND R. J. GOOD. 1987. Monopolar surfaces. Adv. Colloid Interface Sci. 28:35–64.

———, ———, AND ———. 1988. Interfacial Lifshitz-van der Waals and polar interactions in macroscopic systems. Chem. Rev. 88:927–941.

WU, S. 1971. Calculation of interfacial tension in polymer systems. J. Polymer Sci. Part C 34:19–30.

WU, W., R. F. GIESE JR., AND C. J. VAN OSS. 1995. Evaluation of the Lifshitz-van der Waals/acid-base approach to determine surface tension components. Langmuir 11(1):379–382.

ZISMAN, W. A. 1964. Relation to equilibrium contact angle to liquid and solid constitution. Pages 1–51 *in* F. W. Fowkes, ed. American Chemical Society Adv. in Chem. 43:1–51.

———. 1977. Influence of constitution on adhesion. Pages 33–66 *in* Irving Skeist, ed. Handbook of adhesives, 2nd ed. Van Nostrand Reinhold Co., New York, NY.